UTILIZING SPONTANEOUS COILING BEHAVIOR TO INVESTIGATE GAP JUNCTION CHANNELS IN ZEBRAFISH

by

LAURA REICH

A BIOLOGY HONORS THESIS

Presented to the Department of Biology
and the Robert D. Clark Honors College
in partial fulfillment of the requirements for the degree of
Bachelor of Science

June 2020

An Abstract of the Thesis of

Laura Reich for the degree of Bachelor of Science
in the Department of Biology to be taken June 2020

Title: Utilizing spontaneous coiling behavior to investigate gap junction channels in zebrafish

Approved: _____*Adam C. Miller*_____
Primary Thesis Advisor

Animal behavior requires coordination between the nervous and muscular systems. These systems communicate within and between one another at specialized subcellular structures, allowing cells to coordinate their activity to achieve movement. One type of communication used by both systems are gap junction channels (GJCs). GJCs are built by the large Connexin (Cx) family of proteins, which enable direct small molecule exchange between cells. However, it is unknown how individual Cxs contribute to behavior; our goal was to identify the specific Cxs contributing to behavior using genetic and behavioral analyses. We used embryonic zebrafish to address this question due to its genetic access and spontaneous coiling, a behavior requiring GJCs. We developed an automated behavioral tracking system and confirmed its accuracy for quantifying the coiling phenotype of zebrafish using wildtype and *Cx* mutants with muscle defects. Additionally, we performed preliminary antibody staining to identify protein expression of neural Cxs in embryonic zebrafish. Results suggest expression of neural Cxs at neurons required for coiling behavior. Further work will unravel the mechanisms of Cxs in the nervous system and musculature.

Acknowledgements

I would like to thank Professor Adam Miller for challenging me and guiding me during my time in his lab. From brainstorming ideas to providing insight on what it means to be a scientist, he has been an instrumental figure in this process.

I would also like to thank other members of the Miller Lab, particularly Rachel Lukowicz, my mentor during this past year. She has demonstrated immense patience and dedication while teaching me numerous lab techniques and pushing me to think independently. Elliott Abe, of the Niell Lab, also helped tremendously as we learned to use DeepLabCut.

Additionally, I heartily acknowledge the UO Fish Facility Staff for ensuring the proper care of our zebrafish. Staff members, like Tim Mason and Marcy McFadden, have helped this project come to fruition.

I also thank Professor Diana Libuda and Professor Elizabeth Raisanen for serving on my thesis committee. Their insights and support during this process is much appreciated, and I look up to their leadership at the University of Oregon.

Lastly, I would like to thank the Clark Honors College and Biology department for providing me the opportunity to write a thesis. Miriam Jordan's work in coordinating theses within the Clark Honors College does not go unnoticed. The Clark Honors College, as well as the Biology Department, have allowed me to grow as a student, scientist, and critical thinker. I will look upon my time at the University of Oregon fondly.

Table of Contents

List of Figures

Introduction

The nervous system controls behavior in organisms

The nervous system, whether in a zebrafish or a human, holds the key to generating and coordinating an organism's behavior. In order for a zebrafish to swim or a human to ride a bike, they must engage specific neural circuits that drive particular behaviors. While this system appears highly complex, its function is derived by the basic building blocks within it: neurons. The human brain alone contains billions and billions of these building blocks (Pakkenberg & Gunderson, 1988). Neurons are cells, and all cells function in accordance with the tissue they reside within to support and allow for the life of the organism. In the case of neurons, these cells communicate electrically to transmit information throughout the body. Neurons contain several important structures that allow them to move a signal. A neuron typically receives an electrical signal from another cell at its **dendrites**. From here, the electrical signal travels through the cell body to the **axon** and eventually to the axon terminal. The neuron then uses **synapses** to propagate the signal to other cells (Luo, 2015; Figure 1A).

There are two forms of synaptic transmission by which neurons send signals to other cells: chemical and electrical. At chemical synapses, **neurotransmitters** are released from the axon terminal of one neuron into a synaptic cleft, a small space between the cells. This release allows for neurotransmitters to bind to **receptors** on the receiving cell to propel the signal forward. Chemical synapses are unidirectional, in which information travels in one direction. In contrast to the features of chemical synaptic transmission, electrical synapses are directly connected by gap junction

channels (GJCs). These channels allow for the direct flow of **ions** between neurons. Ions can move bidirectionally, allowing for information to propagate in either direction. Furthermore, because of this direct connection between neurons, electrical synapses provide faster transmission of signals than chemical synapses. (Luo, 2015; Figure 1B).

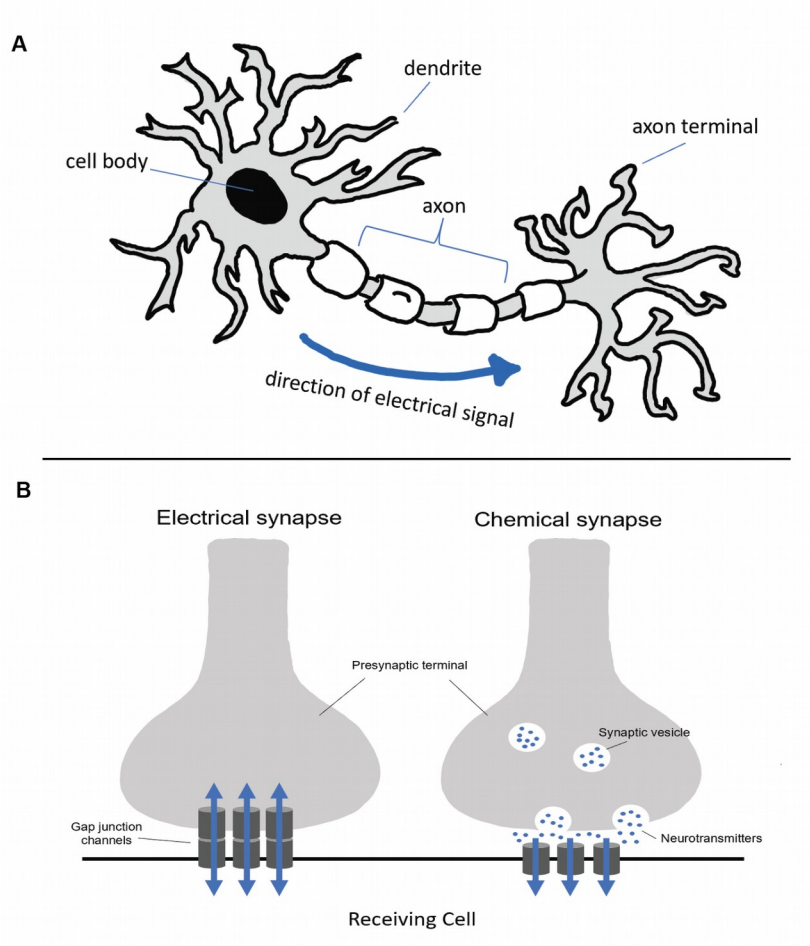

Figure 1. Structure of a neuron and synapses.

(A) An electrical signal is sent to the dendrite of a neuron through synapses. The impulse then moves through its cell body and travels to the axon. The axon terminal contains synapses where the signal is transported to another cell. (B) Electrical synapses are composed of GJCs. Ions flow between cells to carry an electrical current. In chemical synapses, neurotransmitters are released from the synapse of a neuron into the synaptic cleft. The neurotransmitters bind to receptors on the receiving cell to allow the signal to propagate.

These single building blocks, neurons, are typically differentiated into three groups: sensory neurons, interneurons (IN), and motor neurons (MN). Sensory neurons are necessary in transforming environmental stimuli, like a loud noise, into internal electrical impulses that allow the organism to recognize and subsequently respond to its

surroundings. INs connect neurons together in order to propagate a signal, and MNs transmit information from neurons to muscle cells to cause contraction or relaxation (Luo, 2015). These three types of neurons wire together through synapses to create neural circuits necessary for behaviors. Behaviors can be simple and reflexive, like the patellar reflex in humans. When the patellar tendon is stretched, the quadriceps muscle contracts. If a person is standing, this reflex enables the individual to keep their balance and avoid falling backward. A simple neural circuit mediates this response; a sensory neuron extends to and synapses with an IN located in the spinal cord, which in turn reaches out and synapses with an MN that then sends its axon, and the information, back to the quadriceps muscle to elicit contraction (Luo, 2015). Without this simple circuit, this behavior would not exist. Neural circuits are also necessary in complex functions and behaviors, including cognition and emotion (Beauregard & Bourgouin, 2001; Wang, 2013).

Musculature communicates with the nervous system to elicit behavior

While the nervous system may be able to control and coordinate behavior, it requires muscles to carry these behaviors out. As previously mentioned, MNs are instrumental in this process; they send projections from the spinal cord to the muscle (Randall et al., 2002; Eisen, 1991). MNs synapse onto a muscle fiber, transmitting signals to the muscle to initiate contraction or relaxation. There are three types of muscles found in vertebrates: smooth, cardiac, and skeletal muscle. Smooth muscle is found in the walls of hollow organs, and cardiac muscle is solely found in the heart. These both contract rhythmically under involuntary control. In contrast to this, skeletal muscle operates under voluntary control, and it gives rise to the physical movements

and behaviors we observe in an organism (Randall et al., 2002). MNs directly innervate through all three types of muscles to initiate contraction and relaxation in a voluntary or involuntary manner. Through this relationship between the nervous system and musculature, simple and complex behaviors are carried out in an organism.

While the nervous system and musculature must communicate with one another, muscle cells must also be coordinated to other muscle cells to ensure proper function of an organism. One way in which muscles do this is through GJCs. Like the case of electrical synapses, GJCs connect adjacent muscle cells together to allow for the flow of small molecules to propagate information. All muscles contain GJCs except for **differentiated skeletal muscle** (Račkauskas et al., 2010). Smooth and cardiac muscles utilize GJCs because they are electrically coupled and require rapid signal transduction across muscle cells for coordinated contraction and relaxation (Nielson et al., 2012). Previous research also demonstrates that both **fast and slow 'twitch' skeletal muscles** contain GJCs to quickly transmit electrical signals in zebrafish (Hirata, 2012). Hence, GJCs offer a form of communication that occurs in almost all muscle tissue.

Gap junction channels (GJCs) facilitate communication and are comprised of Connexin (Cx) proteins that effect its properties

The nervous and muscular systems contain cells that must communicate with one another, and GJCs are a method of communication utilized by both systems. Thus, a question arises: what are the properties and characteristics of GJCs? GJCs are found in nearly every tissue in an organism, excluding differentiated skeletal muscle, red blood cells, and mature sperm cells (Račkauskas et al., 2010). GJCs function by directly connecting adjacent cells together. This allows for the communication of ions,

secondary messengers, and small metabolites (Meşe & White, 2007). GJCs are formed by two hemichannels that reside within the **plasma membrane** of the respective cells. Hemichannels are composed of six individual proteins. In vertebrates, these are Connexin (Cx) proteins (Račkauskas et al., 2010; Figure 2A).

All Cxs are structurally similar. They are transmembrane proteins, where part of the protein lies within the outer boundary of the cell. Every Cx contains four transmembrane domains, which stretches across the plasma membrane, two extracellular loops which allow for communication with adjacent hemichannels, and one intracellular loop located within the cell. Both the N-terminal and C-terminal, or the ends of the protein, lie inside the cell (Račkauskas et al., 2010; Figure 2B).

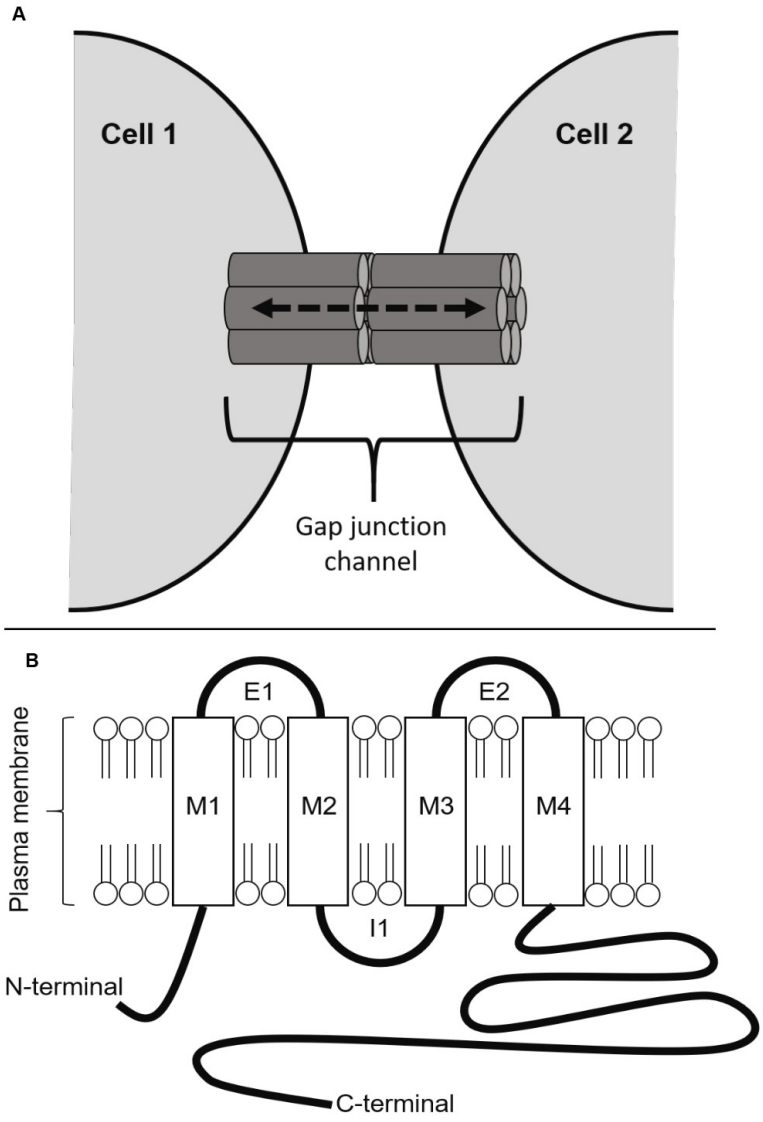

Figure 2. The morphology of GJCs and Cxs.

(A) GJ hemichannels are composed of six Cxs. Two hemichannels from two adjacent cells come together to form the GJC. This allows for the transport of small cytoplasmic molecules, a means of direct electrical and metabolic signaling. The dotted black arrow indicates the flow of small molecules. (B) The Cx is a transmembrane protein with four transmembrane domains (labelled M1, M2, M3, and M4). It also contains two extracellular loops and one intracellular loop (labelled E1, E2, and I1, respectively). Both the N-terminal and C-terminal are located in the inside of the cell. Figure modified from Račkauskas et al., 2010.

The Cx family is a highly conserved, large family with up to 20 Cx-encoding genes in the human **genome** (Eastman et al., 2005). Many Cx-encoding genes demonstrate tissue-type-specific expression, where the gene is expressed in particular organs and cells. For example, *cx36* is found almost exclusively in the nervous system of the majority of mammals (Connors et al., 2004). Additionally, the immense diversity within the Cx family allows for a high degree of specialization in GJCs. Some GJCs are homomeric and are only composed of one type of Cx, while others are heteromeric and are formed by two or more different Cxs. Further still, there are heterotypic GJCs, which are composed of a different set of Cxs on either hemichannel. The molecular composition of a GJC can affect several of its properties. This includes its gating and permeability, which impacts the ability of various ions and small molecules to traverse through the channel (Račkauskas et al., 2010). A number of other factors also regulate GJCs, such as intracellular calcium levels, pH levels, and voltage (Račkauskas et al., 2010). Hence, the composition of GJCs helps determine the molecules that are able to flow through the channel, impacting the way in which cells communicate in a given tissue. Therefore, it is of general interest to identify the Cxs that form a variety of GJCs, especially those relevant to behavior, in order to truly understand how cells work together to achieve an organism's movement.

Zebrafish are a model organism that can be used to further understand the GJCs and Cxs integral to behavior

While it is known that GJCs are important in the coordination of behavior in both the nervous and muscular systems, the specific Cxs that coordinate behaviors are unknown. Zebrafish, specifically embryonic zebrafish, provide a means to study GJCs

and Cxs in vertebrates. Zebrafish have 40 putative Cx-encoding genes, almost twice the number found in mammals (Watanabe, 2017). This is primarily due to a whole genome duplication event that occurred in the **teleost** lineage (Eastman et al., 2005). Despite this, zebrafish are a useful model organism because their genome contains **homologs** for 70% of human protein-coding genes, as well as 84% of genes associated with human disease (Howe et al., 2013). Furthermore, zebrafish develop quickly, are optically translucent, and allow for accelerated genetic studies through gene knockdown and overexpression.

Developing zebrafish contain a model system to study GJC communication within the nervous system and musculature. This model system is the coiling circuit, as it has both neural circuits and muscles containing GJCs (Knogler et al., 2014, Saint-Amant & Drapeau, 2001). However, we do not know the molecular nature nor the precise functional contributions of these various connections. We do know that the coiling circuit is initially composed of MNs and descending interneurons (dIN) that make local electrical synapses within a single segment (Figure 3), and these later connect between segments to coordinate activity along the length of the spinal cord. From here, the MN synapse onto slow muscle fibers that themselves contain GJCs (Figure 3; Knogler et al., 2014; Saint-Amant & Drapeau, 2001).

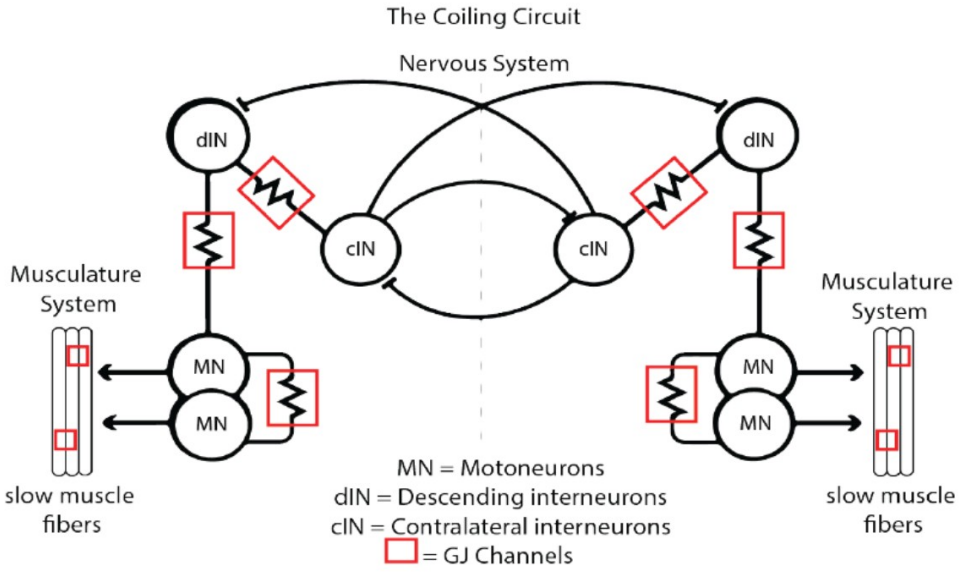

Figure 3. The embryonic zebrafish coiling circuit.

The embryonic zebrafish coiling circuit is composed of dIN neurons, cIN neurons, MN neurons, and slow muscle fibers. Red boxes indicate GJCs. Figure modified from Lukowicz, 2020.

Not only does the coiling circuit contain GJCs in its neurons and musculature, but it also produces a recognizable behavior at 17 hours post fertilization (hpf): spontaneous coiling of the trunk (Figure 4A). This spontaneous coiling occurs from 17 – 26 hpf in the embryonic zebrafish, and coiling increases in angle as the zebrafish develops (Adke, 2018). The frequency of coiling peaks at approximately 19 hpf, and this frequency decreases and eventually disappears after 26 hpf (Saint-Amant & Drapeau, 1998). Spontaneous coiling requires GJCs in the coiling circuit – when chemical inhibitors of GJCs are administered into the embryonic zebrafish spinal cord, there is a loss of the rhythmic neural network activity and coiling behavior (Warp et al., 2012).

The circuit that drives coiling matures and sets up the necessary framework for later behaviors. **Glycine inhibitory chemical synapses** become integrated through **contralateral** interneurons (cIN), and dIN and MN neurons become connected via **glutamate excitatory chemical synapses** (Knogler et al., 2014; Saint-Amant & Drapeau, 2001). As this process takes place, larval zebrafish coiling transitions into a similar yet different behavior at 21 – 28 hpf: touch-evoked coiling. Larval zebrafish then exhibit burst swimming, leading to beat-and-glide swimming at 4 days post fertilization (dpf; Knogler et al., 2014; Figure 4B).

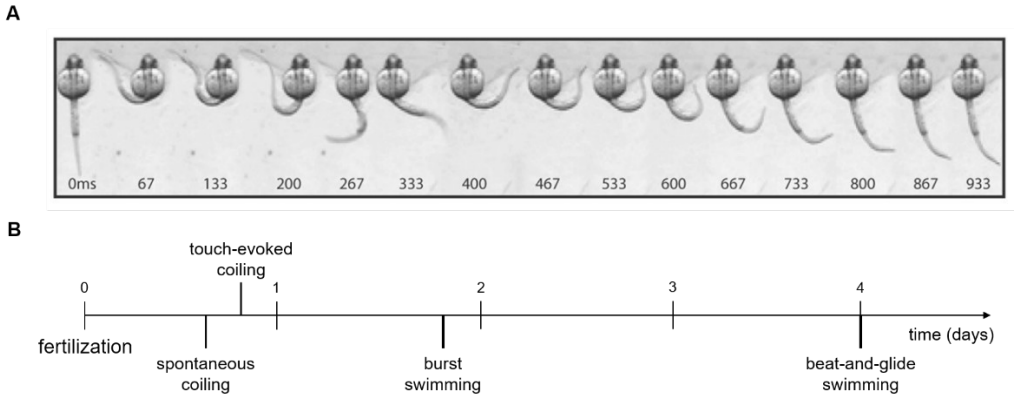

Figure 4. The coiling circuit produces spontaneous coiling and matures to set up the framework for later behaviors.

(A) Coiling in a 26 hpf zebrafish over the course of 933 ms. This behavior is characterized by contraction of the zebrafish's trunk, where the tail extends towards the head of the organism, alternating from left to right. Figure modified from Knogler et al., 2014. (B) Progression of behaviors in embryonic zebrafish during development, beginning with spontaneous coiling at 17 hpf. Modified from Adke, 2018.

Overall, the coiling circuit of the embryonic zebrafish contains GJCs in its neurons and musculature, and it produces a recognizable behavior that requires these GJCs in early development. Thus, the coiling circuit can serve as a model to explore the role of GJCs and identify the specific Cxs necessary for spontaneous coiling.

Previous research in the Miller Lab has investigated the Cxs in the embryonic zebrafish coiling circuit

The zebrafish coiling circuit is a robust model that enables us to study the role of GJCs in the nervous system and musculature. Recognizing this, the Miller Lab sought to identify the Cxs required for spontaneous coiling in the coiling circuit neurons and slow muscle fibers. The Miller Lab utilized **single cell RNA sequencing** (scRNAseq), a method that measures the expression profiles for genes in an individual cell and can be applied to tens of thousands of cells in parallel. The Miller lab used this method to characterize the expression profiles of cells during the first days of zebrafish development (Farnsworth et al., 2019), including at 1 dpf, when the coiling circuit is functional. Analysis of this data grouped cells into clusters based on their similarities in gene expression. We examined this data for MNs and muscles of the early coiling circuit and found that Cx-encoding genes that are **orthologs** of the primary mammalian neural *cx*, *cx36*, are expressed in regions that also show expression of an MN marker. This suggests that these genes (*cx34.1*, *cx35.5*, and *cx35.1*) are producing Cxs that reside at the electrical synapses of MNs in the coiling circuit (Figure 5A). Additionally, we found that *cx46.8* is expressed in regions that also show expression of a slow muscle marker, specifically at 1 dpf (Figure 5B). RNA in-situ hybridization (ISH), a method to visualize gene expression, was performed to corroborate these results. Images from RNA ISH indicate that the pattern of expression of *cx46.8* aligns with slow muscle fibers. Muscle segments of the zebrafish tail appear in a folded, chevron shape, just as the RNA ISH depicts (Rost et al., 2014; Figure 5C).

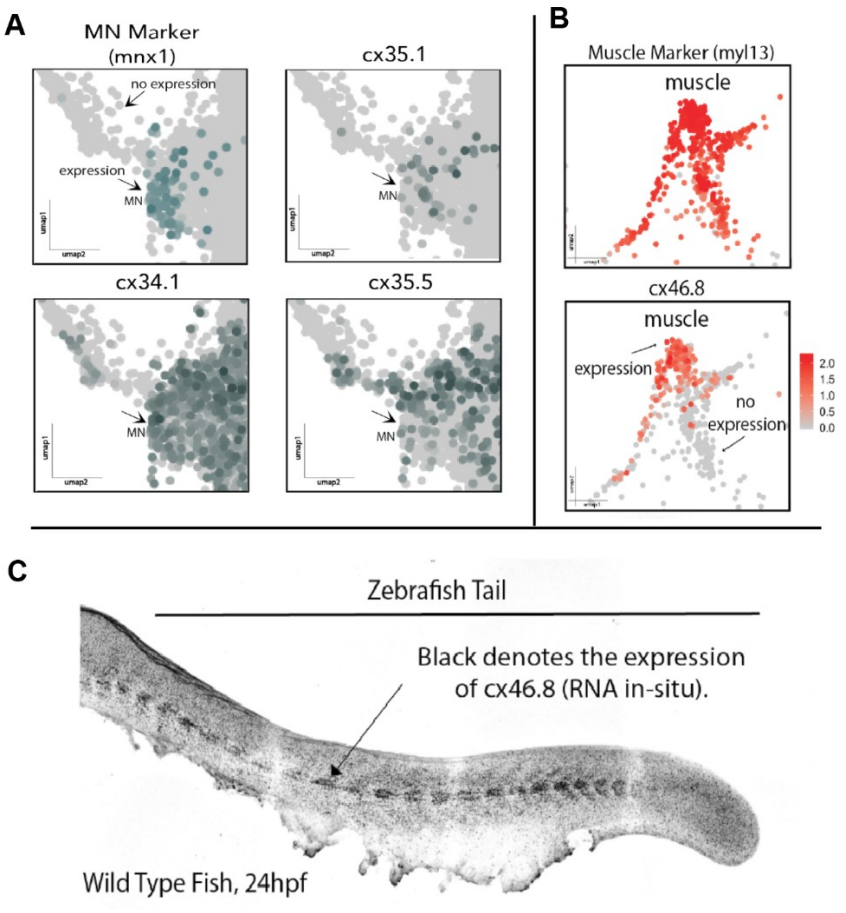

Figure 5. Cx-encoding genes are expressed in MNs and slow muscle fibers of embryonic zebrafish.

(A) scRNAseq expression of *cx35.1*, *cx34.1*, and *cx35.5*. Each dot represents a single cell, and the darkest color represents highest levels of gene expression. *cx34.1* and *cx35.5* show broad expression, whereas *cx35.1* shows limited expression. MN Marker shows the expression of a marker for motor neurons. Figure modified from Lukowicz, 2020. B) scRNAseq expression of *cx46.8*, where each dot represents a single cell. Dark red indicates the highest levels of corresponding gene expression. The expression of a known slow-twitch muscle marker appears in the top box, whereas *cx46.8* expression is shown in the bottom box. C) *cx46.8* RNA ISH, depicting muscle expression in black. Figure modified from Lukowicz, 2020.

The Miller Lab wanted to determine if these identified Cx-encoding genes are required for spontaneous coiling. Using Clustered Regularly Interspaced Short Palindromic Repeats (CRISPR), a tool used to edit genomes, the Miller Lab disrupted

cx46.8 and found that the mutant exhibited a behavioral defect in spontaneous coiling. The lab then propagated this line and characterized the mutation, an 8 base pair deletion at the cut site (Adke, 2018). Initial behavioral analysis was performed on **Homozygous** *cx46.8* mutants (*cx46.8*$^{-/-}$), and they found that these mutants exhibit a weak and asymmetric coiling across development compared to **wild-type** (WT) siblings, although the frequency of coiling is the same (Figure 6). Thus, not only is *cx46.8* found in slow muscle fibers, it is required for proper spontaneous coiling.

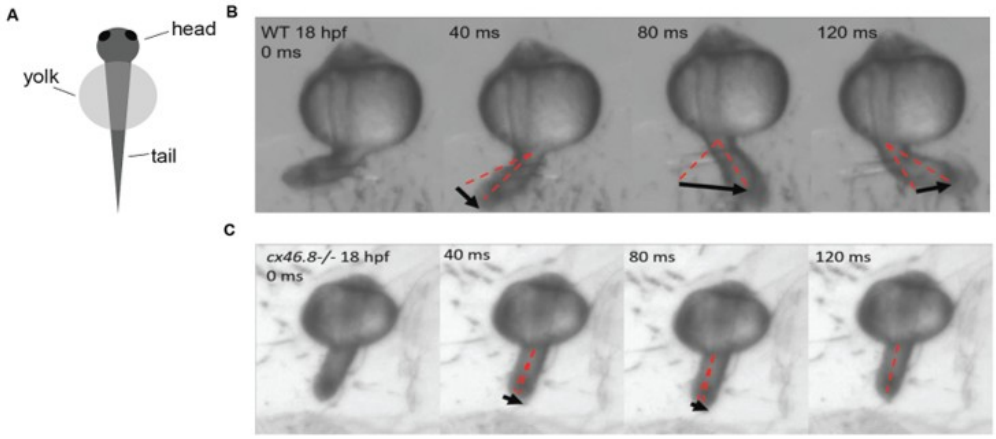

Figure 6. *cx46.8*$^{-/-}$ zebrafish exhibit defects in coiling.

(A) Orientation of embryonic zebrafish in (B and C). The zebrafish is placed with its ventral side upwards. (B and C) Coiling over time in WT and *cx46.8*$^{-/-}$ zebrafish at 18 hpf. The coiling angle of the mutant is much smaller. Dotted red lines indicate movement of the zebrafish tail over the 40-millisecond interval. Black arrows indicate the direction of movement over the 40-millisecond interval.

Overall, this research has provided a framework for identifying the Cxs of the coiling circuit that are required for spontaneous coiling. The data from scRNAseq suggests that several Cx-encoding genes, including *cx36* orthologs, are expressed in coiling neurons in early development. Previous research shows that neural Cxs, particularly Cx34.1 and Cx35.5, are expressed in the spinal cord at 5 dpf (Miller et al.,

2017). As a next step to this, we sought to determine if these neural Cxs are present in coiling circuit neurons at 24 hpf, and in the big picture, whether they control function. In addition, scRNAseq data demonstrates that *cx46.8* is expressed in slow muscle. RNA ISH confirms these results. The Miller Lab also disrupted *cx46.8* and screened for perturbations in coiling behavior to understand how this specific Cx contributes to the coiling circuit. With this previous research in mind, the overarching goal now is to develop and then utilize a sensitive and high-throughput behavioral tracking system to screen Cx-encoding genes to determine their role in the circuit. We intend to generate an automated tracking system to track spontaneous coiling because manual tracking would be time-consuming, inefficient, and error-prone; researchers are required to measure and analyze changes in organism position through their own judgment. Furthermore, we can validate the efficiency of a new tracking system with *cx46.8*$^{-/-}$ mutants, as it is known through preliminary manual behavioral analysis that they exhibit a behavioral defect (Adke, 2018). Thus, the coiling circuit is a model system that enables us to further the research of the Miller Lab and understand the characteristics of Cxs in the nervous system and musculature's coordination of behavior.

Research Aims

The goal of this thesis was to expand our understanding of how GJCs and Cxs aid in coordination of behaviors through the nervous system and musculature. We focused on the coiling circuit of embryonic zebrafish to do this. We first aimed to build a high-throughput, automated behavioral tracking system to further elucidate the genes associated with GJCs that are critical for spontaneous coiling. In addition to behavioral tracking, we performed a series of molecular pilot experiments to identify proteins

associated with the GJCs in coiling circuit cells. We used DeepLabCut (DLC), a **3D markerless pose estimator**, to generate an automated tracking system that will serve as a high-throughput tool to quantify coiling behavior in larval zebrafish (Mathis et al., 2018; Nath et al., 2018). We validated the efficiency of DLC by comparing coiling behavior in WT and *cx46.8*$^{-/-}$ zebrafish because a behavioral phenotype was already known (Adke, 2018). Next, preliminary antibody staining was performed on 24 hpf zebrafish to determine if Cxs used in other neural circuits are used in the early coiling circuit (Miller et al., 2017). These techniques, both behavioral and molecular, were constructed and utilized for the future prospect of using them as screening platforms to determine the involvement of additional Cxs in the circuit and its behavioral output. Overall, this thesis furthers the research of the Miller Lab by continuing to understand the importance of Cxs and GJCs through behavioral and molecular means.

Results

Creating an automated behavioral tracking system to analyze spontaneous coiling

To further understand the role of Cxs in coiling behavior, we trained DLC, a high-throughput system, to track the tail movement of WT and *cx46.8*$^{-/-}$ zebrafish. This not only allowed us to further examine the coiling phenotype of WT and *cx46.8*$^{-/-}$ zebrafish, but it also allowed us to create a screening platform to analyze the behavior of other mutants. As a first step in this process, we set up embryonic zebrafish for behavioral imaging. We embedded larval zebrafish in 1.4% low-melt agarose on their back. The zebrafish, still embedded in low-melt agarose, were then placed in a petri dish filled with embryo medium (EM). The zebrafish were adjusted to be ventral side up, and using tweezers, the agarose was removed around the tail to allow for full tail movements (Figure 7A). The petri dish was positioned on a transparent plastic panel with a camera directly below the panel for video capture to take place (Figure 7C and 7D). To maintain consistency in lighting conditions, a single light source was placed above the petri dish. A fogged plastic panel was placed between the dish and light source to avoid glare (Figure 7B). This behavioral set-up allows for adequate imaging, as seen in Figure 7A. The agarose keeps the zebrafish restrained while still allowing for movement of its tail. The lighting conditions enable us to differentiate the zebrafish from the agarose and EM, and we can move the petri dish without adjusting the camera position (Figure 7C and 7D).

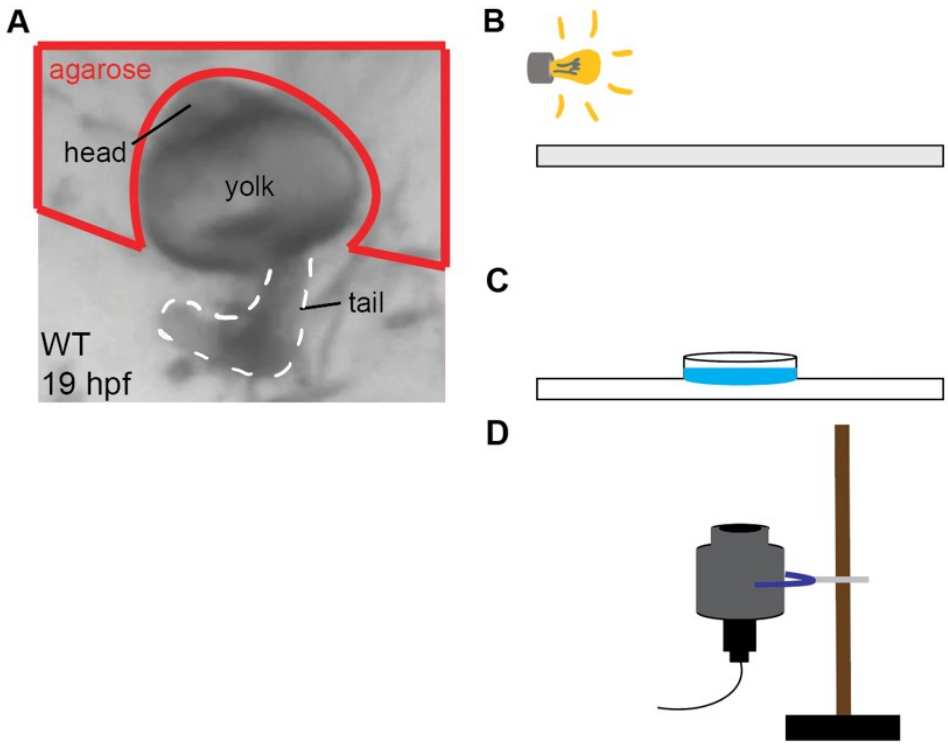

Figure 7. Experimental set-up enables imaging of spontaneous coiling.

(A) WT zebrafish at 19 hpf, ventral side up, embedded in 1.4% low-melt agarose and placed in a petri dish filled with EM. The tail is freed from agarose to allow for uninhibited spontaneous coiling. Areas in the image with agarose are designated by the red outline. White dashed lines indicate the region of the tail. (B) Fogged panel (12" by 18") placed above petri dish and camera to filter light from small light source. (C) Petri dish with zebrafish embedded in agarose placed on top of transparent plastic panel. (D) Sentech camera and lens suspended by clamp and ring stand. The Sentech camera was connected to a computer with Mightex Systems software v1.2.1 (computer not shown).

With a method for behavioral imaging established, we trained a neural network (DLC) to automatically track the movements of the zebrafish tail. A neural network, in general, is a series of algorithms that can learn to perform tasks based on examples it is provided. In our case, DLC is a neural network that we intend to train to recognize and track the movement of coiling behavior. We aim to train DLC so that if it is provided a novel video of coiling, it will be able to track the coiling behavior accurately. The

process of DLC training was divided into 3 steps, where (1) we captured 150 frames of video of WT animals throughout coiling behavior (18 – 21 hpf), (2) we manually defined biologically relevant points on each frame, and (3) we trained the DLC network on the University of Oregon Talapas Supercomputer (Figure 8A). We used 4 different videos of WT zebrafish coiling behavior to extract 150 frames. These videos were consistent in their lighting conditions, but slight alterations were made to make the DLC training network versatile in its tracking. Of these 4 videos, 2 were representative of early development (18 – 19 hpf), while the other 2 videos were representative of later development (21 – 22 hpf). Even within this 4-hour time frame, the tail of the zebrafish lengthens and the coiling phenotype changes slightly (Knogler et al., 2014). Furthermore, the zebrafish in these 4 videos were imaged with slightly different orientations. Although all zebrafish were imaged ventral side up with their tail towards the bottom of the frame, some zebrafish were turned (Figure 8B). Again, these slight changes in videos aimed to create a versatile DLC training network, which will be more equipped to track coiling behavior on novel videos with slight variations in the zebrafish's developmental age and spatial orientation. With the 4 videos chosen, 150 frames were randomly extracted. We manually defined 6 points on each frame: the top of the head, the two sides of the yolk, as well as the beginning, middle, and end of the tail (Figure 8C). We chose to establish points at the top of the head and the sides of the yolk as stable points to ensure that DLC can recognize a lack of movement. We defined points for the start, middle, and end of tail to understand how the different regions of the tail move during spontaneous coiling. Once points were manually established, the DLC network was trained on the University of Oregon Talapas Supercomputer.

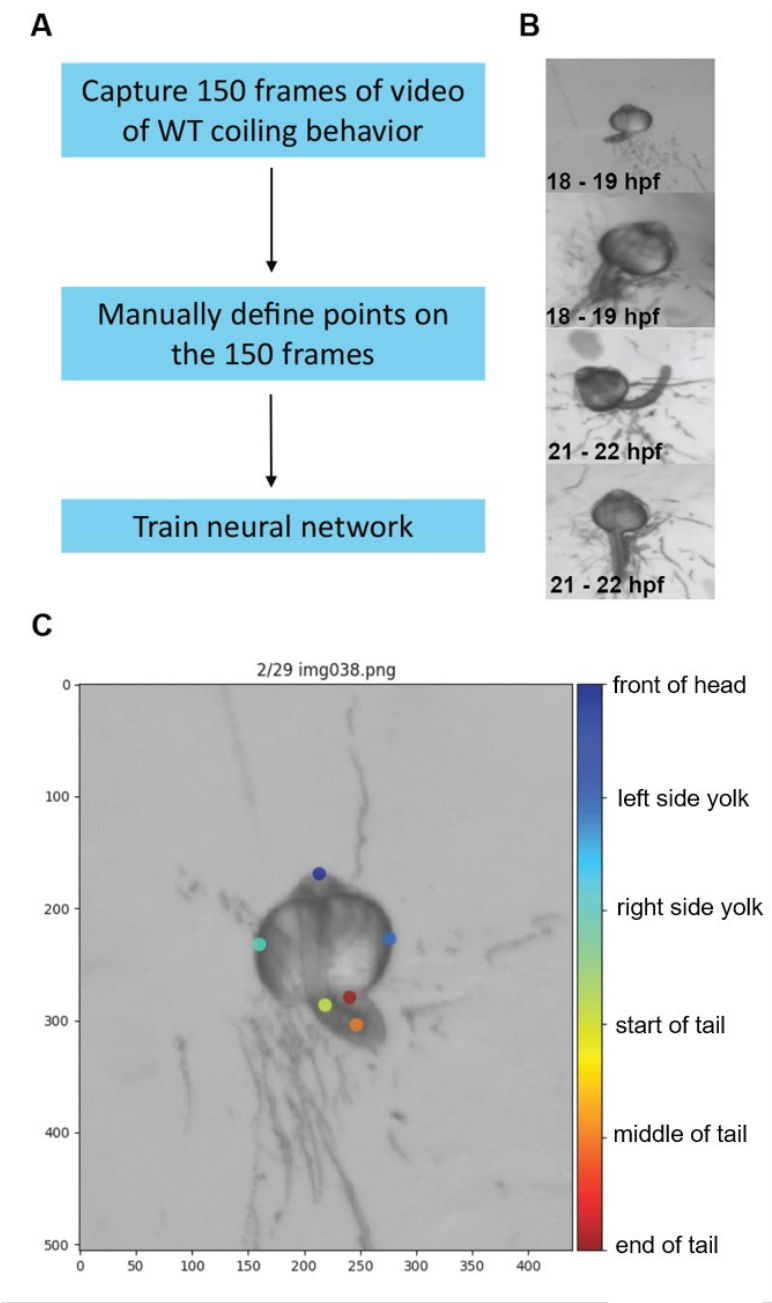

Figure 8. The DLC network must be trained to track spontaneous coiling.

(A) Training of the DLC network comprised of 3 steps, whereby 150 frames were extracted from videos of WT coiling behavior, points were manually defined on the frames, and the network was trained. (B) Images from the 4 videos used to train the DLC network, with 2 representing 18 – 19 hpf and 2 representing 21 – 22 hpf. Each video comprised of a different zebrafish at a slightly different orientation. (C) 6 points were manually defined on each frame. The points were defined as follows: front of head, left side yolk, right side yolk, start of tail, middle of tail, and end of tail.

Once the DLC network was trained, we wanted to examine if the network properly tracks tail movement from a novel video of zebrafish coiling. Novel videos of WT coiling behavior were given to the network, and the network then analyzed the videos by estimating the position of the 6 defined points onto each novel frame. From the analysis, the network provides an annotated video with the placed labels, as well as a trajectory plot indicating the movement of these points over the course of the video (Figure 9). Furthermore, the network outputs the precise X and Y coordinates of each defined point in each given frame. The DLC neural network was able to track the points with little error when given a 25 second video of zebrafish coiling behavior. The DLC network recognizes a lack of movement on the upper half of the zebrafish, including the top of the head and the yolk, as well as the beginning of the tail (Figure 9). The network also recognizes movement at the middle of the tail and end of the tail (Figure 9A and 9C). However, not every video was tracked perfectly. Discrepancies in tracking were most likely to occur in the tracking of the end of the tail (Figure 9B and 9D). This may be due to several reasons. First, zebrafish embryos are transparent, and the end of the tail can be especially difficult to differentiate with the background due to the lighting contrast. Additionally, because the end of the tail is experiencing the largest change in position over time, the DLC network may struggle to identify it. Despite these inconsistencies, the DLC neural network is still able to recognize stationary regions of the organism, including the top of head and sides of yolk, as well as recognize movement in the different regions of the tail. For example, Figure 9C depicts a span of about 80 pixels of the end of the tail for an 18 hpf WT zebrafish, and Figure 9D displays a span of about 100 pixels for a 19 hpf WT zebrafish.

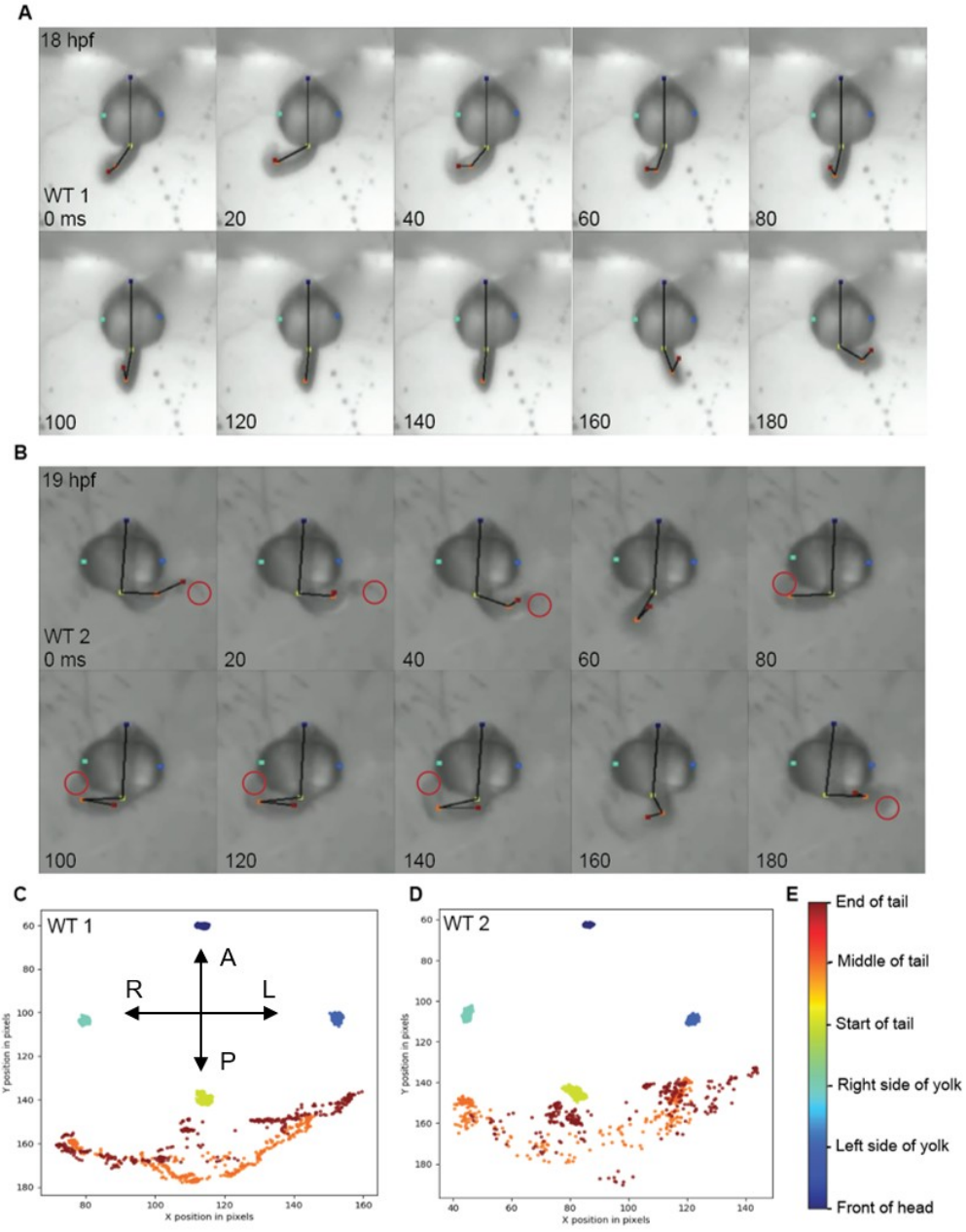

Figure 9. The trained DLC network tracks spontaneous coiling.

(A) 180 millisecond (ms) time lapse of DLC tracking of WT zebrafish at 18 hpf. Each colored dot represents a point tracked by the DLC software. Black line tracks change in points between top of head through the end of the tail. (B) 180 ms time lapse of DLC tracking of a different WT zebrafish at 19 hpf. Red circle indicates actual position of the end of the tail. (C) Trajectory plot of 25 second video from (A). Each dot indicates position of that point in a frame of the video. Axis of orientation indicates that the anterior (A) portion of the fish lies upwards, posterior (P) downwards, and left (L) and right (R) in opposite directions, based on the zebrafish's point of view. (D) Trajectory plot of 25 second video from (B). (E) The color of each point designates a different part of the zebrafish body the neural network is intending to track.

In order to compare WT coiling behavior to *cx46.8*$^{-/-}$ coiling behavior, behavioral imaging was performed across development, between 18 – 21 hpf. Over the course of this time period, 25 second videos were recorded at 30-minute intervals. We subsequently gave these videos to the DLC network, wherein it tracked the 6 points based on its training. Figure 10A depicts the tracking of a WT zebrafish at 4 different time points. The angle of coiling becomes wider for this particular WT zebrafish through its development. At 18 hpf, the end-of-tail has a range of about 30 pixels at the X-axis; this range expands to about 130 pixels at 21 hpf. In contrast to this, trajectory plots from a single *cx46.8* mutant depicts a much smaller span of the end-of-tail (Figure 10B). At 18 hpf, the end-of-tail remains close to the 100-pixel position of the x-axis with little movement. This movement does expand, but the span of the end-of-tail only reaches about 50 pixels at 21 hpf. Additionally, based on the trajectory plots of this single mutant, asymmetric coiling is apparent, where the mutant coils predominantly towards its right side.

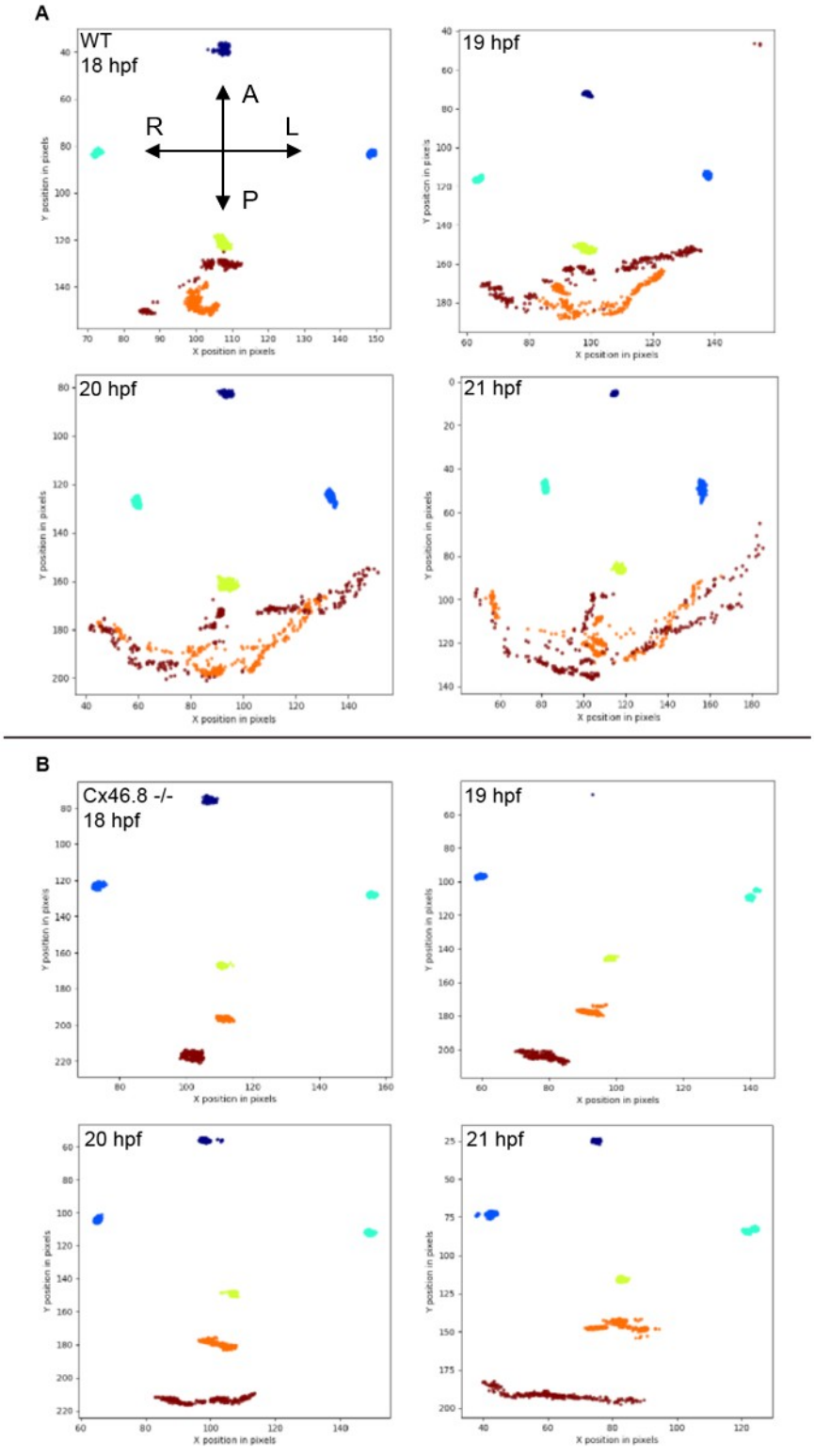

Figure 10. DLC trajectory plots show the tail movement of individual WT and *cx46.8*$^{-/-}$ zebrafish coiling.

(A) Trajectory plots of single WT zebrafish based on 25 second videos taken at every hour, determined by DLC tracking. (B) Trajectory plot of single *cx46.8*$^{-/-}$ zebrafish based on 25 second videos at every hour, determined by DLC tracking. Colors coincide with legend in Figure 9E. Axis of orientation indicates that the anterior (A) portion of the fish lies upwards, posterior (P) downwards, and left (L) and right (R) in opposite directions, based on the zebrafish's point of view.

Initial tracking and trajectory plots from the trained DLC network provide promising data that suggests weaker and asymmetric coiling in *cx46.8* mutant zebrafish. While trajectory plots of single zebrafish provide us with an initial depiction of coiling behavior, it does not compare and quantify the coiling behavior of multiple zebrafish. Data comparison and quantification of coiling behavior will determine the behavioral defects of *cx46.8*$^{-/-}$ zebrafish with certainty. This will confirm the accuracy of the system and its potential use as a screening platform for other mutants of Cx-encoding genes.

Behavioral analysis from tracked spontaneous coiling behavior shows potential to systematically assess coiling phenotypes

We successfully trained a high-throughput system to track spontaneous coiling in WT and *cx46.8*$^{-/-}$ zebrafish. However, the DLC tracking does not provide a means to directly compare tracking between videos. Initial behavioral analysis in the Miller Lab indicate that *cx46.8*$^{-/-}$ zebrafish exhibit weak and asymmetric coiling without perturbations in coiling frequency (Adke, 2018). We sought to further analyze and compare tracked DLC data points from both WT and *cx46.8*$^{-/-}$ videos to corroborate these results. This will demonstrate the training network's ability as an efficient screening platform that can lead to analysis of behavioral defects in other mutants for Cx-encoding genes.

First, we normalized the DLC data points. This allows for comparison between zebrafish with slight variation in size and resting position. With the normalized data, we plotted the middle-of-tail and end-of-tail X-coordinate over time for one WT and one *cx46.8*$^{-/-}$ zebrafish in early and late development (Figure 11). We specifically focused on the X-coordinate to determine if phenotypic differences are still apparent between zebrafish in a simplified comparison. All X-coordinate positions in the positive direction indicate tail movement towards the right, whereas X-coordinate positions in the negative direction indicate tail movement to the left. Figure 11 demonstrates that 1) *cx46.8*$^{-/-}$ exhibit smaller changes in tail movement at the X-coordinate at both 18 and 21 hpf and 2) the frequency at which the X-coordinate oscillates is similar between WT and *cx46.8*$^{-/-}$. This suggests that *cx46.8*$^{-/-}$ zebrafish are attempting to coil just as frequently as WT controls, but the coils of the mutants are weaker. Furthermore, early in development, both the WT and *cx46.8*$^{-/-}$ zebrafish exhibit a higher frequency of coils than later in development. Hence, through a simplified comparison of X-coordinates, we confirm that *cx46.8*$^{-/-}$ coil more weakly, yet at the same frequency, as WT.

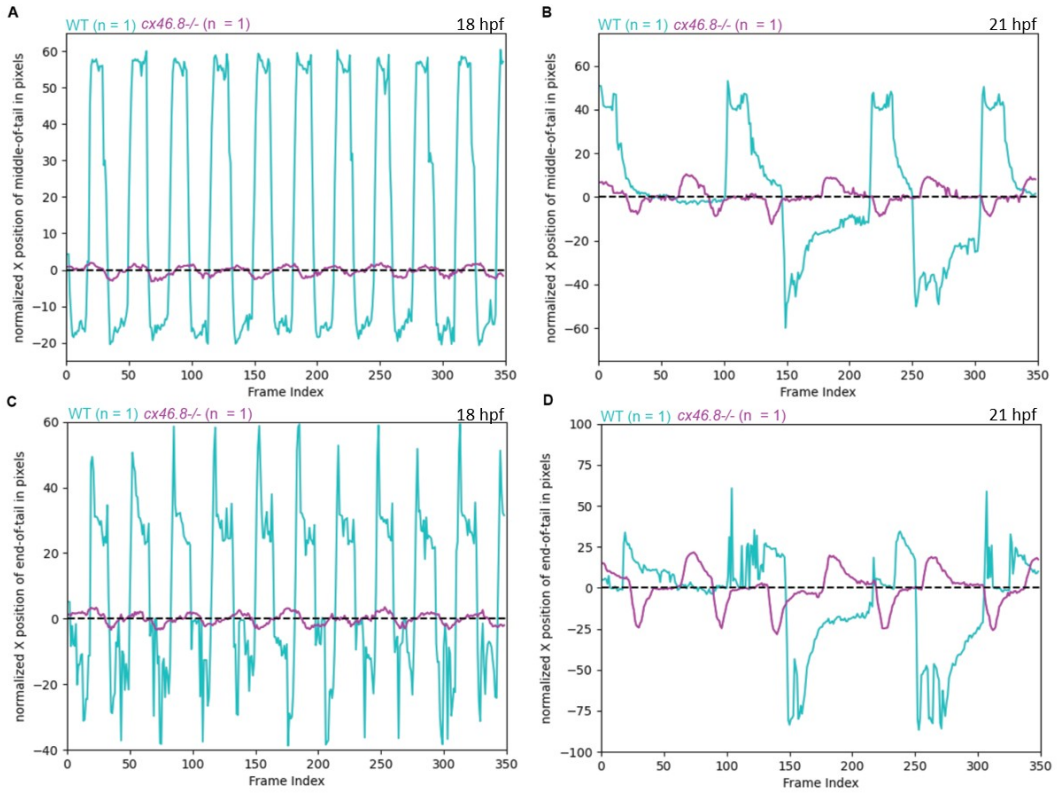

Figure 11. *cx46.8*$^{-/-}$ zebrafish exhibit weaker coiling and similar frequency of coils compared to WT.

(A and B) The normalized position of the middle-of-tail X-coordinate over the course of 350 frames, approximately 25 seconds, for both a representative WT (cyan) and *cx46.8*$^{-/-}$ (magenta) zebrafish at 18 and 21 hpf, respectively. (C and D) The normalized end-of-tail X coordinate over the course of 350 frames for WT and *cx46.8*$^{-/-}$ at 18 and 21 hpf, respectively.

Figure 11 directly compares the movement of the middle-of-tail and end-of-tail for two zebrafish over time. We then devised a method to increase our sample size of comparison by generating box-and-whisker plots. These box-and-whisker plots show the distribution of the X-coordinate over the course of development in WT and *cx46.8*$^{-/-}$ zebrafish (Figure 12). A smaller distribution of the X-coordinate indicates a smaller range of movement by the zebrafish. This serves to confirm the weaker coiling of

cx46.8$^{-/-}$ zebrafish. At all measured time points in development, the distribution of the X-coordinate at the middle-of-tail and end-of-tail was smaller in *cx46.8*$^{-/-}$ zebrafish (Figure 12).

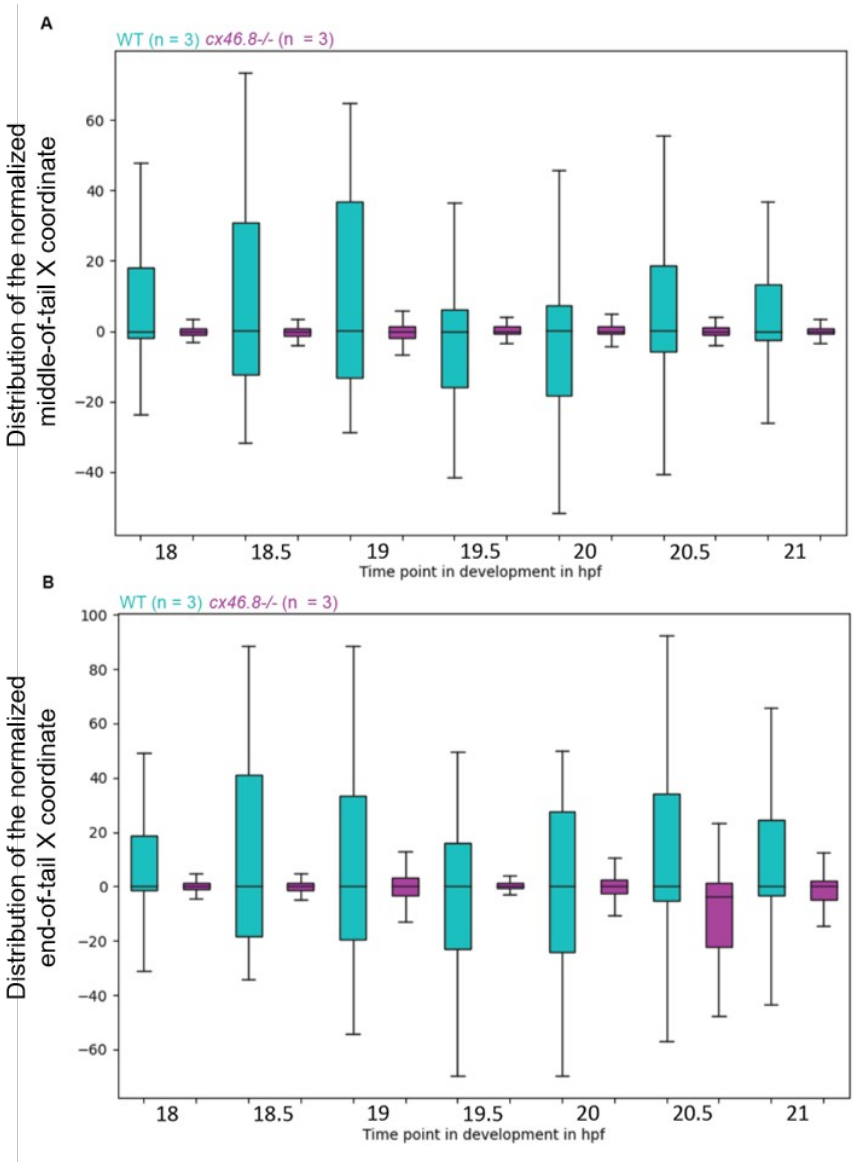

Figure 12. *cx46.8*$^{-/-}$ zebrafish exhibit weaker coiling across development.

(A and B) Distribution of the normalized middle-of-tail and end-of-tail X-coordinate for WT and *cx46.8*$^{-/-}$ zebrafish across development. Box-and-whisker plots denote the mean X-coordinate, 25th and 75th percentiles, as well as the non-outlier minimum and maximum values.

Lastly, we sought to confirm that *cx46.8*$^{-/-}$ attempt to coil at the same frequency as WT using a larger sample size. We counted the peaks of tail movement through plots similar to Figure 11. Each oscillatory peak was counted as an attempted coil. Results indicate that across development, WT and *cx46.8*$^{-/-}$ coil at similar frequencies and show a decrease in coiling frequency over time, corroborating previous research (Figure 13; Adke, 2018; Saint-Amant & Drapeau, 1998).

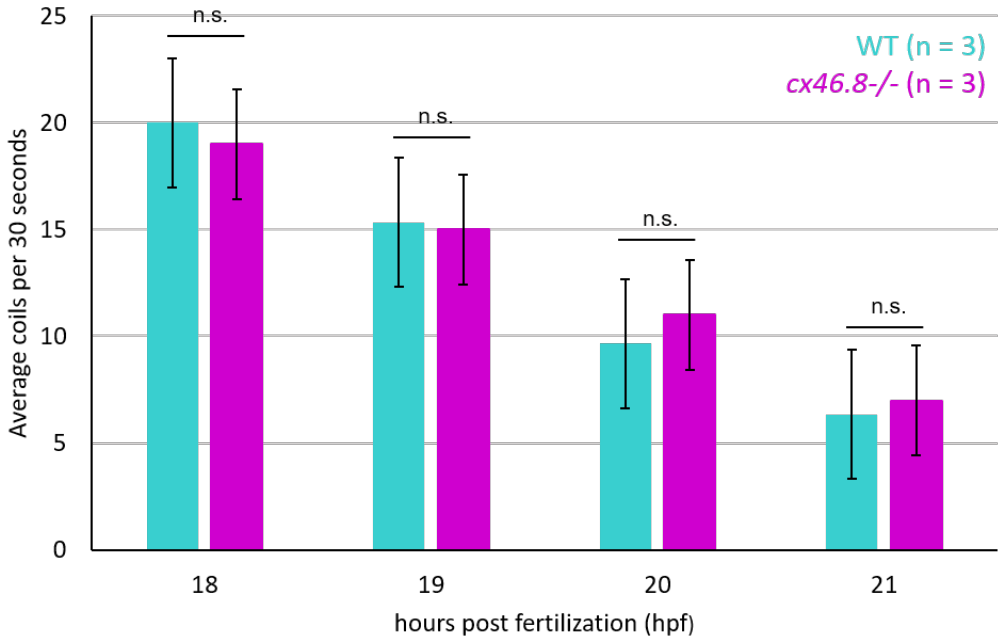

Figure 13. WT and *cx46.8*$^{-/-}$ zebrafish attempt to coil at the same frequency.

From 18 – 21 hpf, both WT and *cx46.8*$^{-/-}$ zebrafish exhibit coiling behavior at a similar frequency, with the number of coils decreasing as the zebrafish develop. There is no significant difference (n.s.) between attempted coiling frequency at each time point ($p > 0.05$, one-way ANOVA). Error bars represent standard error.

Using the data provided by the trained DLC network, we are able to quantify and compare phenotypic differences in WT and *cx46.8*$^{-/-}$ zebrafish across development. This preliminary quantification of coiling behavior indicates that *cx46.8*$^{-/-}$ exhibit weaker coiling at the same frequency as WT, confirming previous behavioral analysis

in the Miller Lab (Adke, 2018). Furthermore, quantification shows a decline in coiling frequency across development, also shown through previous research (Saint-Amant & Drapeau, 1998). This confirms the accuracy of our trained network and its robust ability to analyze spontaneous coiling. In addition, this paves the way for its use as a screening platform to investigate the role of other Cx-encoding genes in the coiling circuit.

Antibody staining suggests localization of Cx36 orthologs within coiling circuit neurons

The goal of our developed tracking software is to systematically analyze zebrafish coiling behavior, with the bigger goal of allowing us to observe changes in mutants that affect the behavior and therefore underly the functional connectivity of the circuit. Above, we confirmed the accuracy of our tracking system using WT and *cx46.8*$^{-/-}$ zebrafish. It is known that *cx46.8* is expressed in slow muscle and is required for proper spontaneous coiling. However, the coiling circuit neurons are also heavily coupled through Cx-mediated GJCs. Yet, the molecular identity of the Cxs that form these neural connections is not yet known. The Miller Lab performed scRNAseq analysis and found that *cx36* fish orthologs are expressed at the same cell cluster as a MN marker, suggesting that they reside in coiling circuit neurons. To confirm if the proteins of these genes are localized in coiling circuit neurons, we performed preliminary antibody staining on 24 hpf zebrafish using the antibody for Cx36, the primary neuronal Cx in mammals, which is known to recognize the Cx36 fish orthologs (Cx34.1, Cx35.5, Cx34.7, and Cx35.1) (Miller et al., 2017). We used a transgenic line that captures endogenous oligodendrocyte transcription factor (Olig2) expression through green fluorescent protein (GFP). Olig2 is a protein that localizes to neurons

within the coiling circuit (Park et al., 2002). Using this system, we can visualize some of the coiling circuit neurons and determine if Cx36 orthologs localize at the cell membrane, providing the first hint of the molecular identity of the Cx-forming coiling circuit electrical synapses. Initial imaging captured expression at single slices of the Z-plane, which is a single, 2-dimensional image within a portion of the 3-dimensional organism. We also captured max projections, which show the expression patterns from all captured Z-plane slices. There is a large amount of puncta staining from Cx36, particularly in the max projection (Figure 14C). However, when viewing a single slice of the zebrafish olig2+ cells, there is high intensity Cx36 puncta signal at the cell membrane, suggesting the potential for localization of Cx36 orthologs within coiling circuit neurons, which was previously unknown (Figure 14B).

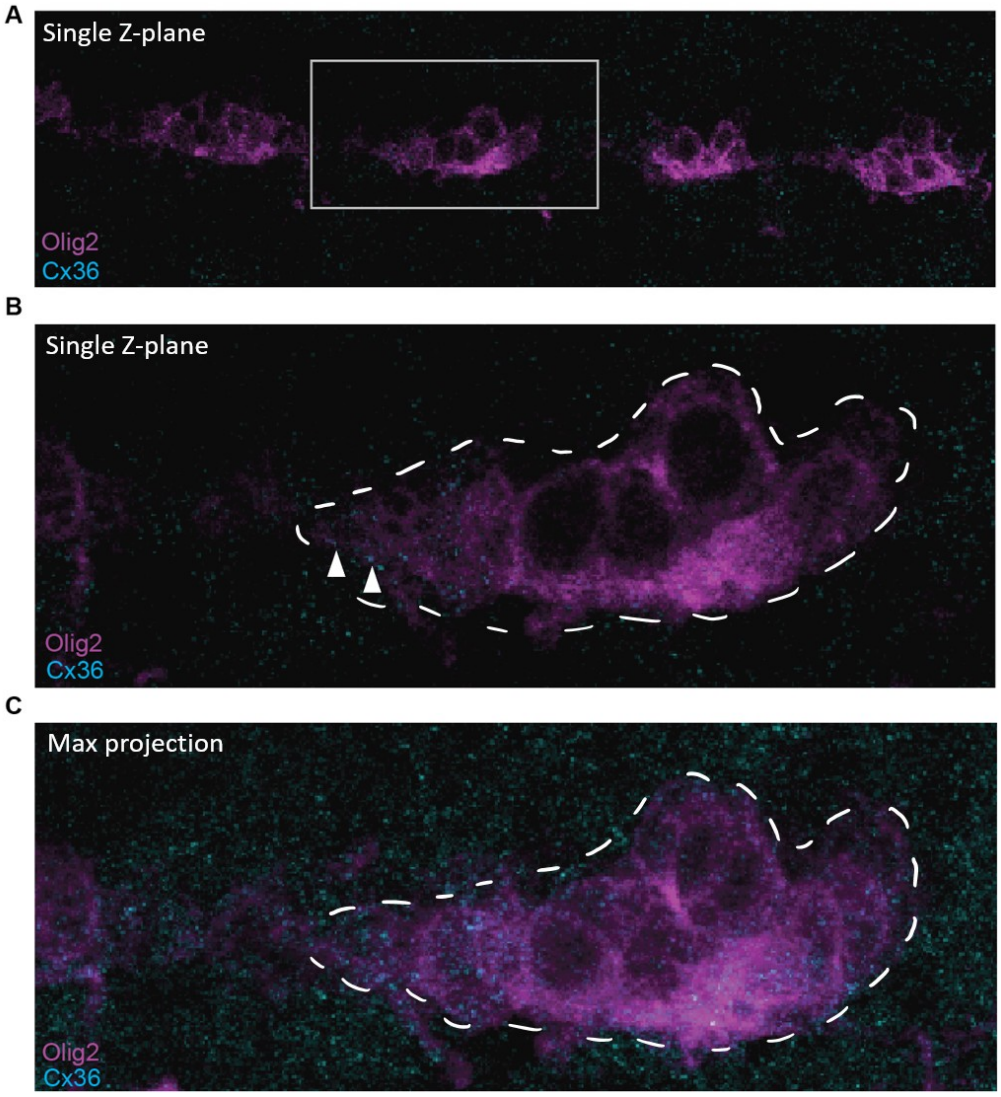

Figure 14. Antibody staining suggests expression at the embryonic zebrafish spinal cord.

(A) Slice of staining of Olig2 and Cx36 in the anterior of a 24 hpf zebrafish. The grey box surrounds the area shown in (B and C). (B) Slice of enlarged portion from (A). White arrowheads indicate potential localization of Cx36 (cyan) at the cell membrane. Dashed lines depict the cell cluster of interest, captured through the olig2 transgenic line. (C) Max projection of enlarged segment of (A). Dashed lines depict cell cluster of interest.

Previous research demonstrates that Cx36 orthologs, most notably Cx35.5 and Cx34.1, are utilized in zebrafish neural circuits at 5 dpf (Miller et al., 2017). However, prior to this, we did not know if the same group of Cxs were being utilized in young and different circuits. Our preliminary antibody staining provides evidence that Cx36 orthologs are localized within some coiling circuit neurons in 1 dpf zebrafish. This indicates that neuronal Cxs, whether Cx35.5, Cx34.1, Cx35.1, and/or Cx34.7, are likely comprising the GJCs within the electrical synapses of coiling circuit neurons. While our studies with DLC and *cx46.8*$^{-/-}$ solidified the importance of the GJCs in the musculature for the proper output of spontaneous coiling, preliminary antibody staining highlights that neuronal Cxs in the coiling circuit also play a role in controlling and coordinating behavior.

Discussion

The purpose of this thesis was to utilize behavioral and molecular techniques to investigate the GJCs and Cxs required for spontaneous coiling. GJCs form critical structures in both the nervous system and musculature, which communicate in order to coordinate activity and achieve movement. Thus, this thesis focused on both systems by investigating the role of *cx46.8*, a Cx-encoding gene known to be expressed in slow muscle, as well as neural Cxs, such as Cx34.1 and Cx35.5. We sought to create an automated screening platform to measure spontaneous coiling, since manual behavioral tracking is time-consuming, inefficient, and error-prone. We trained a DLC network to track the movement of the larval zebrafish tail and confirmed the accuracy of this system by analyzing videos of WT and *cx46.8*$^{-/-}$ zebrafish, both previously studied in the Miller Lab (Adke, 2018). Behavioral analysis using DLC data confirms that *cx46.8*$^{-/-}$ zebrafish coil more weakly, yet at the same frequency as WT zebrafish. Additionally, analysis indicates that coiling frequency decreases over the course of development in both WT and *cx46.8*$^{-/-}$ zebrafish, which has been characterized in WT zebrafish in previous research (Saint-Amant & Drapeau, 1998). The Miller Lab additionally found asymmetric coiling in *cx46.8*$^{-/-}$ zebrafish. While this was not analyzed thoroughly within our data analysis, DLC trajectory plots of individual *cx46.8*$^{-/-}$ mutants do indicate asymmetry of tail movement (Figure 10B). Overall, we trained a DLC network that adequately tracks tail movement in embryonic zebrafish. This DLC network paves the way for a screening platform to measure the coiling phenotype of other mutants because of its accuracy and efficiency. This allows us to further characterize Cxs required for spontaneous coiling and the coiling circuit.

While our work using DLC focuses on a Cx-encoding gene expressed in slow muscle fibers, we also sought to explore the importance of neural Cxs in spontaneous coiling. After all, spontaneous coiling requires coordination between the coiling circuit and associated musculature. We performed preliminary antibody staining on 24 hpf zebrafish to explore the expression of neural Cxs in the spinal cord and coiling circuit using a human Cx36 marker. Staining indicates the potential expression of neural Cxs, such as Cx34.1 and Cx35.5, at GJCs near cell clusters of the spinal cord. Previous research in the Miller Lab found neural Cx expression in the spinal cord at 5 dpf (Miller et al., 2017). Our antibody staining provides evidence that neural Cxs are expressed in the spinal cord as early as 1 dpf. Altogether, this thesis highlights the complex interaction and coordination between muscles and neurons. GJCs and their Cxs, whether in the nervous system or musculature, allow for effective communication and elicitation of behaviors for the proper function of an organism.

Future Directions

There are numerous future directions that extend from this thesis. First, to optimize behavioral analysis, we plan to measure zebrafish development based on somite count instead of hpf. The time course of zebrafish development can vary depending on the individual zebrafish or zebrafish line (Stickney et al., 2000). Previous research in the Miller Lab did note developmental delays in *cx46.8*$^{-/-}$ mutants (Adke, 2018). Thus, using somite count will increase the accuracy in our assessment of coiling phenotype at specific developmental timepoints. Second, while the DLC training network is generally able to track the movement of a larval zebrafish tail, we intend to fine-tune tracking. For example, the end of the tail is difficult to track in some videos (Figure 9B). DLC is an active-learning-based network that can be refined as it is exposed to more videos and fine-tuned by the user (Nath et al., 2018). This work will not only improve data analysis of WT and *cx46.8*$^{-/-}$ zebrafish, but it will also enable the network to become a screening platform for other mutants of Cx-encoding genes, including mutants for the *cx36* fish orthologs. Furthermore, one particular Cx, Cx39.9, is also known to localize to slow muscle fibers in zebrafish, and assessment of the coiling phenotype of mutants for its associated gene could further our understanding of the role of GJCs in muscle (Hirata et al., 2012).

While we can improve the DLC training network, we can also consider alternative methods to investigate the role of Cx46.8 in zebrafish. We have yet to analyze behavioral features of *cx46.8*$^{-/-}$ after 24 hpf, when spontaneous coiling ceases. There may be alterations in the phenotype of later behaviors, such as touch-evoked coiling, burst swimming, or beat-and-glide swimming. Examining these behaviors can

expand our understanding of this protein's necessity and role in slow muscle fibers of the coiling circuit as it matures.

There are several avenues of research that extend from our work and analysis on the coiling phenotype, but we also intend to continue using molecular techniques to study Cxs of the coiling circuit. Antibody staining of the human Cx36 marker demonstrated the potential for neural Cx expression in the spinal cord of 24 hpf zebrafish. Performing antibody staining on another set of 24 hpf zebrafish can help confirm this. Furthermore, we can perform RNA in-situ hybridization of the Cx-encoding genes of neural Cxs. This will determine the gene expression of Cx-encoding genes at the spinal cord and coiling circuit neurons. This research will broaden our knowledge of GJCs associated specifically with the neurons of the coiling circuit.

By understanding and recognizing the specific Cxs that comprise GJCs of the coiling circuit, we gain knowledge about the ways in which the nervous system and musculature communicate within and between their systems to coordinate activity and achieve an organism's movement. A lack of proper coordination between the nervous and muscular systems can be detrimental to the overall function and survival of an organism. While our research is focused on Cxs within embryonic zebrafish, we can use this knowledge to further understand the coordination of these two systems in other organisms, such as humans. Some human disorders might arise from improper function and localization of Cxs; our research can serve as a foundation for future therapeutic strategies that treat movement disorders.

Method Details

Animal use and care

Zebrafish used for experiments were bred and raised using standard protocols and procedures ascribed by the University of Oregon Institutional Animal Care and Use Committee (Westerfield, 2000). Zebrafish lines used, including control lines (m/colo GFP-) and *cx46.8* del8bp mutants (GFP-), were light-cycle shifted by 5 hours. Embryos were born at 3 pm, with behavioral imaging occurring from 9 am (18 hpf) to 1 pm (22 hpf). Zebrafish of the Tg(olig2:GFP) line were used for antibody staining; they were not light-cycle shifted, and they were reared under standard conditions.

Behavioral imaging and analysis

Behavioral imaging took place in a room held at a constant temperature of 28°C, optimal for zebrafish growth and development (Westerfield, 2000). The chorion of the embryo was removed with tweezers at 17 hpf. Embryos were embedded within 1.4% low-melt agarose in EM. Embryos within agarose were placed on a petri dish and oriented with their ventral side facing upwards. Embryo medium was added to the petri dish, and the agarose surrounding the tail of the embryo was removed with tweezers. Videos were recorded using the Sentech STC-MBA5MUSB3 with the Kipon Canon EOS-C lens. Mightex Systems software v1.2.1 was used to adjust video settings, including the start and end of the video. Each video was approximately 30 seconds long with a resolution of 2592 H x 1944 V and a frame rate of 60 FPS. Videos were recorded every 30 minutes between 9 am and 1 pm. Behavioral imaging set-up is depicted in Figure 7.

DLC was downloaded and installed through github, and Python was utilized to import the training videos and 6 defined frames into the DLC network. DLC training of the neural network, “MountedComplete,” took place on the University of Oregon Talapas Supercomputer for 8 hours.

The tracked points determined by DLC in each video that were processed through the neural network were further analyzed, normalized, and plotted using Matplotlib in Python. Points were normalized by selecting the median of the point of interest, either the middle-of-tail or end-of-tail point. Statistics, specifically the one-way analysis of variance (one-way ANOVA) was performed using Excel.

Antibody staining

Zebrafish of the Tg(olig2:GFP) line were euthanized with MESAB at 24 hpf. Embryos were removed from their chorion using tweezers. Following this, embryos were fixed in 2% TCA, diluted in PBS with Triton-X100 (PBSTx) for 3 hours, rocking at room temperature. Embryos were then dissected to remove their yolks. Afterwards, they were washed 5 times in PBSTx at 5-minute intervals. Once these washes were complete, the embryos were blocked using Western block solution for 20 minutes. Western block solution was then replaced with diluted primary solution. Primary solution contained anti-mouse Cx36, anti-chicken GFP, and anti-rabbit isl1/2. The fish were rocked in this solution at room temperature overnight.

Primary solution was taken off the fish and the embryos were washed 5 times in PBSTx for at least 15 minutes. The embryos were then incubated in secondary solution, wrapped in foil, and set to rock in room temperature for 2 hours. Secondary solution contained rabbit antibody, mouse antibody, chicken antibody, and DAPI. The antibodies

responded to wavelengths of 633 nm, 594 nm, and 488 nm, respectively. The embryos were washed 5 times in PBSTx, for at least 15 minutes each, and underwent step-wise dehydration to 75% glycerol. Afterwards, the embryos were mounted on a glass slide and imaged using a Leica confocal microscope. Images taken with the microscope were analyzed and processed afterwards using ImageJ.

Glossary

3D markerless pose estimator: a network that is able to estimate the location and movement of a 3D object without manually marking the object

axon: the long segment of a neuron where an electrical impulse moves to be transmitted to another cell

contralateral: on opposite sides; in the embryonic spinal cord, contralateral neurons are on opposite sides of the neural circuit

dendrite: the branched extension of a neuron that typically receives an electrical impulse from its synapses

differentiated skeletal muscle: skeletal muscle with single muscle cells that have fused together to form a myotube and contains multiple cell nuclei

fast and slow 'twitch skeletal muscles: fast 'twitch' skeletal muscle is important for powerful bursts of movement, while slow 'twitch' skeletal muscle is important for long-endurance use

genes: a sequence of the DNA that encodes for the synthesis of a gene product, such as a protein

genome: the entire genetic material of an organism

glutamate excitatory chemical synapse: a type of chemical synapse that uses glutamate as a neurotransmitter; activity at this synapse excites cells connected to it

glycine inhibitory chemical synapse: a type of chemical synapse that uses glycine as a neurotransmitter; activity at this synapse inhibits cells connected to it

homolog: a gene inherited by two species that comes from a common ancestor

homozygous: when the two alleles for a gene are identical

ions: molecules that have an overall negative or positive charge

neurotransmitter: molecule used in chemical synapses to carry a signal from one cell to another

ortholog: gene sequences that are similar and found in different species related by linear descent

plasma membrane: the outer boundary of a cell; it is comprised of a lipid bilayer with a number of proteins and other molecules that help regulate processes of the cell, including transport

receptors: chemical structures that receive and send signals within biological systems

single cell RNA sequencing: a technique that examines the quantity and sequences of RNA (a molecule that carries information from DNA for the synthesis of proteins) in a single cell

synapse: a junction between two neurons that allows for a signal to move from one neuron to another

teleost: a large group of fish descending from the same evolutionary lineage

transgenic: an organism that contains genetic material that has been artificially introduced from an unrelated organism

wild-type: a strain or gene that is prevalent in normal populations of an organism; it is often used as a control

References

Adke, A., & Miller, A. (2018). The Genetic Basis for the First Connections in the Brain (Unpublished undergraduate thesis). University of Oregon.

Beauregard, M., Le, J., & Bourgouin, P. (2001). *Neural Correlates of Conscious Self-Regulation of Emotion*. *21*, 1–6.

Connors, B. W., & Long, M. A. (2004). Electrical Synapses in the Mammalian Brain. *Annual Review of Neuroscience*, *27*(1), 393–418. https://doi.org/10.1146/annurev.neuro.26.041002.131128

Eastman, S. D., Chen, T. H. P., Falk, M. M., Mendelson, T. C., & Iovine, M. K. (2006). Phylogenetic analysis of three complete gap junction gene families reveals lineage-specific duplications and highly supported gene classes. *Genomics*, *87*(2), 265–274. https://doi.org/10.1016/j.ygeno.2005.10.005

Eisen, J. S. (1991). Motoneuronal development in the embryonic zebrafish. *Development*, *113*(SUPPL. 2), 141–147.

Farnsworth, D.R. et al. (2019), A single-cell transcriptome atlas for zebrafish development, Developmental Biology, https://doi.org/ 10.1016/j.ydbio.2019.11.008

Hirata, H., Wen, H., Kawakami, Y., Naganawa, Y., Ogino, K., Yamada, K., … Kuwada, J. Y. (2012). Connexin 39.9 protein is necessary for coordinated activation of slow-twitch muscle and normal behavior in zebrafish. *Journal of Biological Chemistry*, *287*(2), 1080–1089. https://doi.org/10.1074/jbc.M111.308205

Howe, K., Clark, M.D., Torroja, C. F., Torrance, J., Berthelot, C., Muffato, M., Collins, J.E. Humphray, S., McLaren, K., Matthews, L., … Chow, W, D. L. (2013). The zebrafish reference genome sequence and its relationship to the human genome. *Nature*, *496*(7446), 498–503. https://doi.org/10.1038/nature12111

Knogler, L. D., Ryan, J., Saint-Amant, L., & Drapeau, P. (2014). A Hybrid Electrical/Chemical Circuit in the Spinal Cord Generates a Transient Embryonic Motor Behavior. *Journal of Neuroscience*, *34*(29), 9644–9655. https://doi.org/10.1523/jneurosci.1225-14.2014

Luo, L. (2015). *Principles of Neurobiology*. New York, NY: Garland Science. doi: 10.1201/9781317553830

Mathis, A., Mamidanna, P., Cury, K. M., Abe, T., Murthy, V. N., Mathis, M. W., & Bethge, M. (2018). DeepLabCut: markerless pose estimation of user-defined body parts with deep learning. *Nature Neuroscience*, *21*(9), 1281–1289.

Meşe, G., Richard, G., & White, T. W. (2007). Gap junctions: Basic structure and function. *Journal of Investigative Dermatology*, *127*(11), 2516–2524. https://doi.org/10.1038/sj.jid.5700770

Miller, A. C., Whitebirch, A. C., Shah, A. N., Marsden, K. C., Granato, M., O'Brien, J., & Moens, C. B. (2017). A genetic basis for molecular asymmetry at vertebrate electrical synapses. *ELife*, *6*. https://doi.org/10.7554/elife.25364

Nath, T., Mathis, A., Chen, A. C., Patel, A., Bethge, M., & Mathis, M. W. (2018). Using DeepLabCut for 3D markerless pose estimation across species and behaviors. *BioRxiv*, 476531. https://doi.org/10.1101/476531

Nielson et al. (2012). Gap Junctions. *Compr Physiology*; 2(3). doi:10.1002/cphy.c110051.

Pakkenberg, B. and Gundersen, H.J.G. (1988), Total number of neurons and glial cells in human brain nuclei estimated by the disector and the fractionator. *Journal of Microscopy*, 150: 1-20. doi:10.1111/j.1365-2818.1988.tb04582.x

Park, H. C., Mehta, A., Richardson, J. S., & Appel, B. (2002). Olig2 Is Required for Zebrafish Primary Motor Neuron and Oligodendrocyte Development. *Developmental Biology*, *248*(2), 356–368. https://doi.org/10.1006/dbio.2002.0738

Račkauskas, M., Neverauskas, V., & Skeberdis, V. (2010). Diversity and properties of connexin gap junction channels. *Medicina, 46*(1), 1. https://doi.org/10.3390/medicina46010001

Račkauskas, M., Verselis, V. K., & Bukauskas, F. F. (2007). Permeability of homotypic and heterotypic gap junction channels formed of cardiac connexins mCx30.2, Cx40, Cx43, and Cx45. *American Journal of Physiology - Heart and Circulatory Physiology*, *293*(3), 1729–1736. https://doi.org/10.1152/ajpheart.00234.2007

Randall, D. J., Burggren, W. W., French, K., & Eckert, R. (2002). *Eckert animal physiology: Mechanisms and adaptations*. New York: W.H. Freeman and Co.

Rost, F., Eugster, C., Schröter, C., Oates, A. C., & Brusch, L. (2014). Chevron formation of the zebrafish muscle segments. *Journal of Experimental Biology*, *217*(21), 3870–3882. https://doi.org/10.1242/jeb.102202

Saint-Amant, L., & Drapeau, P. (1998). Time course of the development of motor behaviors in the zebrafish embryo. *Journal of Neurobiology*, *37*(4), 622–632. https://doi.org/10.1002/(SICI)1097-4695(199812)37:4<622::AID-NEU10>3.0.CO;2-S

Saint-Amant, L., & Drapeau, P. (2001). Synchronization of an Embryonic Network of Identified Spinal Interneurons Solely by Electrical Coupling. *Neuron*. *31*, 1035–1046.

Stickney, H. L., Barresi, M. J. F., & Devoto, S. H. (2000). Somite Development in Zebrafish. *Developmental Dynamics*, *303*(July), 287–303. https://doi.org/10.1002/1097-0177(2000)9999:9999<::AID-DVDY1065>3.0.CO;2-A

Watanabe, M. (2017). Gap junction in the teleost fish lineage: Duplicated connexins may contribute to skin pattern formation and body shape determination. *Frontiers in Cell and Developmental Biology*, *5*(FEB), 1–8. https://doi.org/10.3389/fcell.2017.00013

Wang X-J (2013) The prefrontal cortex as a quintessential "cognitive-type" neural circuit: working memory and decision-making. Principles of Frontal Lobe Function, Edited by DT Stuss and RT Knight, Second Edition, Cambridge University Press, pp. 226-248.

Warp, E., Agarwal, G., Wyart, C., Friedmann, D., Oldfield, C. S., Conner, A., … Isacoff, E. Y. (2012). Emergence of patterned activity in the developing zebrafish spinal cord. *Current Biology*, *22*(2), 93–102. https://doi.org/10.1016/j.cub.2011.12.002

Waterhouse, J. (2008). Muscle Types. *Anasthesia and Intensive Care Medicine*, *9*(6), 264–269. doi:10.1016/j.mpaic.2008.04.011

Westerfield, M. (2000). The zebrafish book. A guide for the laboratory use of zebrafish (Danio rerio). 4th ed., Univ. of Oregon Press, Eugene.